MOLECULAR AND CELLULAR BIOLOGY, Jan. 2011, p. 30–42 Vol. 31, No. 1
0270-7306/11/$12.00 doi:10.1128/MCB.00648-10

Nek10 Mediates G_2/M Cell Cycle Arrest and MEK Autoactivation in Response to UV Irradiation▽

Larissa S. Moniz[1]† and Vuk Stambolic[1,2]*

Department of Medical Biophysics, University of Toronto, Toronto, Ontario M5G 2M9, Canada,[1] and Division of Signaling Biology, Ontario Cancer Institute, University Health Network, Toronto, Ontario M5G 2M9, Canada[2]

Received 3 June 2010/Returned for modification 24 June 2010/Accepted 11 October 2010

Appropriate cell cycle checkpoint control is essential for the maintenance of cell and organismal homeostasis. Members of the Nek (NIMA-related kinase) family of serine/threonine protein kinases have been implicated in the regulation of various aspects of the cell cycle. We explored the cellular functions of Nek10, a novel member of the Nek family, and demonstrate a role for Nek10 in the cellular UV response. Nek10 was required for the activation of extracellular signal-regulated kinase 1/2 (ERK1/2) signaling upon UV irradiation but not in response to mitogens, such as epidermal growth factor stimulation. Nek10 physically associated with Raf-1 and MEK1 in a Raf-1-dependent manner, and the formation of this complex was necessary for Nek10-mediated MEK1 activation. Nek10 did not affect the kinase activity of Raf-1 but instead promoted the autophosphorylation-dependent activation of MEK1. The appropriate maintenance of the G_2/M checkpoint following UV irradiation required Nek10 expression and ERK1/2 activation. Taken together, our results uncover a role for Nek10 in the cellular response to UV irradiation.

The Nek kinases (NIMA-related kinases) are a family of cell cycle-regulated serine/threonine kinases. The founding member of the family, *Aspergillus nidulans* NIMA (never in mitosis A) is essential for mitotic entry (23). Based on the amino acid homology within their respective catalytic domains, 11 mammalian Nek kinases have been identified (16), and many have been shown to play diverse roles both during mitosis and at the other phases of the cell cycle. In addition to their roles during normal cell cycle progression, recent work has implicated specific Nek family members in checkpoint control and the DNA damage response.

For instance, by directly phosphorylating the CDK1-activating phosphatase Cdc25A, Nek11 enhances its interaction with the E3 ubiquitin ligase SCF β-TrCP, promoting its degradation (17). Consistent with a key role of Cdc25A degradation in the induction of cell cycle arrest following genotoxic stress, Nek11-depleted HeLa cells exhibit elevated levels of the Cdc25A protein and fail to undergo ionizing radiation (IR)-induced G_2/M arrest (17). Also, in HeLa cells, IR inactivates Nek2, which appears to be essential for the radiation-induced inhibition of centrosome splitting (20). Conversely, Nek1 expression and catalytic activity are elevated in HK2 and HeLa cells treated with IR (25), and kat2J/Nek1$^{-/-}$ cells were deficient in their ability to repair DNA following this genotoxic stress (7). Finally, the catalytic activities of Nek1, Nek2, Nek6, and Nek11 appear to be sensitive to genotoxic stresses such as UV radiation, IR, and etoposide (10, 15, 22, 25). Thus, various Nek kinases participate in the cellular response to genotoxic stress and can act as positive and negative regulators of various damage-induced checkpoints.

Many cellular stresses, including UV irradiation, lead to the activation of the mitogen-activated kinases Jun N-terminal protein kinase (JNK), p38, and extracellular signal-regulated kinase 1/2 (ERK1/2). While UV-induced JNK activation leads to a primarily proapoptotic response, p38 is required for the engagement of the G_2/M checkpoint (3, 31, 34). The physiological relevance and the mechanism of ERK1/2 activation in response to UV irradiation are less well characterized. Nevertheless, the activation of ERK1/2 is emerging as an important aspect of G_2/M checkpoint control in a cell type- and stimulus-specific manner. For instance, ERK1/2 activation by IR and etoposide in MCF7 and NIH 3T3 cells is required for G_2/M arrest (30, 32).

Here, we explore the cellular functions of human Nek10, a novel member of the Nek family and a recently identified candidate susceptibility gene in breast cancer and other cancers (1, 8, 11). Our results demonstrate a role for Nek10 in the maintenance of the G_2/M checkpoint following UV irradiation. Mechanistically, Nek10 was found to act as a positive regulator of ERK1/2 signaling in response to UV irradiation, but not mitogenic stimuli, by forming a complex with Raf-1 and MEK1 and enhancing MEK1 autoactivation. Importantly, our data indicate that Nek10 may regulate the UV-induced checkpoint in mammalian cells.

MATERIALS AND METHODS

All materials were obtained from Sigma unless otherwise indicated. UV irradiation (254 nm) was performed by using a UV Stratalinker 2400 instrument (Stratagene, La Jolla, CA).

Plasmids. Nek10 cDNA was isolated by PCR from a skeletal muscle cDNA library (HL5505u; Clontech) based on the longest predicted Nek10 transcript (16) and was confirmed by sequencing. The resulting cDNA was subcloned into the EcoRI and KpnI sites of 3× FLAG-CMV-7.1. Deletion mutants of Nek10 were generated by standard recombinant DNA procedures (details are available upon request). Catalytically inactive Nek10 (kinase dead [KD]) was generated by the site-directed mutagenesis of lysine 548 to arginine. pEBG-Raf-1 was pro-

* Corresponding author. Mailing address: Princess Margaret Hospital, 10th Floor, Rm. 10-123, 610 University Ave., Toronto, Ontario M5G 2M9, Canada. Phone: (416) 946-2961. Fax: (416) 946-2985. E-mail: vuks@uhnres.utoronto.ca.

† Present address: Centre for Cell Signalling, Institute of Cancer, Queen Mary University of London, Charterhouse Square, London EC1M 6BQ, United Kingdom.

▽ Published ahead of print on 18 October 2010.

vided by J. Woodgett. Catalytically inactive Raf-1 (KD) was generated by site-directed mutagenesis of lysine 375 to tryptophan. pMCL HA-MEK1 was provided by M. Cobb, and pcDNA HA-MEK1, MEK1 K97A (KD), MEK1 Δ270-307, V5-Pak1, and Pak1 K299R (KD) were provided by A. Catling.

Cell culture and transfection. HEK293 cells were cultured in Dulbecco's modified Eagle's medium (DMEM)–10% fetal bovine serum (FBS), and plasmids were transfected by using the calcium phosphate method. MCF7 cells were cultured in DMEM–10% FBS, and MCF10A cells were cultured in DMEM-F12 medium supplemented with 5% horse serum, epidermal growth factor (EGF) (20 ng/ml), hydrocortisone (0.5 mg/ml), cholera toxin (100 ng/ml), and insulin (10 μg/ml). MCF7 and MCF10A cells were transfected with Effectene (Qiagen) according to the manufacturer's instructions. For knockdown using endoribonuclease prepared small interfering RNA (esiRNA), cells were transfected with Dharmafect 1 (Dharmacon) according to the manufacturer's instructions. Briefly, 1 to 2 μg of esiRNA was transfected per 35-mm plate on day 1 and day 2. Medium was changed 24 h following transfection. For semiquantitative reverse transcription (RT)-PCR, RNA was extracted on day 3. For fluorescence-activated cell sorter (FACS) analysis, cells were gathered on day 4. For the preparation of whole-cell lysates, cells were lysed on day 4 (48 h following transfection).

Cell lysis and immunoprecipitation. Cells were lysed in CHAPS {3-[(3-cholamidopropyl)-dimethylammonio]-1-propanesulfonate} lysis buffer (40 mM HEPES [pH 7.5], 0.5% CHAPS, 120 mM NaCl, 1 mM EDTA, 50 mM NaF, 1 mM Na_2VO_3, 20 mM β-glycerophosphate, 1 mM dithiothreitol [DTT], and protease inhibitors). Immunoprecipitations were performed with anti-Flag M2-agarose or glutathione-Sepharose 4 Fast Flow (GE Healthcare) for 2 h at 4°C, washed four times with CHAPS lysis buffer containing 220 mM NaCl, and eluted by boiling in sample buffer. V5 immunoprecipitations were performed with anti-V5 antibody and protein G-Sepharose. Hemagglutinin (HA) immunoprecipitations were performed with anti-HA 12CA5 and protein G-Sepharose for 2 h at 4°C, washed one time with CHAPS lysis buffer containing 400 mM NaCl and one time with CHAPS lysis buffer, and eluted by boiling in sample buffer.

Western blot analysis and antibodies. Whole-cell lysates or immunoprecipitates were resolved by SDS-PAGE and blotted onto polyvinylidene difluoride (PVDF) membranes. Proteins were probed by using appropriate primary antibodies from the following sources: anti-ERK1/2 (catalog number 9102), anti-phospho-ERK1/2 (T202/Y204) [anti-pERK1/2 (T202/Y204)] (catalog number 9101), anti-pMEK1/2 (S217/221) (catalog number 9121), anti-pMEK1/2 (S298) (catalog number 9128), anti-pp38 (T180/Y182) (catalog number 9211), anti-pJNK1/2 (T183/T185) (catalog number 9251), and anti-pRaf-1 (S338) (catalog number 9427) were obtained from Cell Signaling; anti-Raf-1 (C20) (catalog number sc-227) was obtained from Santa Cruz; antivinculin was obtained from Abcam; anti-Flag M2 was obtained from Sigma; anti-glutathione *S*-transferase (anti-GST) was obtained from GE Healthcare; anti-V5 was obtained from Invitrogen; and anti-HA 12CA5 was harvested from the supernatant of the corresponding hybridoma.

***In vitro* kinase assay. (i) Nek10 and Pak kinase assays.** Flag-Nek10 or V5-Pak1 immunoprecipitates were washed two times with CHAPS lysis buffer plus 0.4 M LiCl and two times with Nek10 kinase assay buffer (KAB) (50 mM MOPS [morpholinepropanesulfonic acid] [pH 7.4], 10 mM $MgCl_2$, 10 mM $MnCl_2$, 2 mM EGTA, 20 mM β-glycerophosphate, 1 mM DTT). Kinase assays were performed with a 40-μl reaction mixture containing 30 μl KAB supplemented with 5 μM ATP and 5 μCi [γ-^{32}P]ATP and either recombinant histone H3 (0.4 μg), GST–Raf-1 (Δ1-306,Y340/341D) (GST–Raf-1 TA) (0.5 μg) (Millipore), or GST-MEK (1.0 μg) (Millipore). Reactions were carried out for 30 min at 30°C and stopped with SDS loading buffer. Reaction mixtures were separated by SDS-PAGE and detected by autoradiography.

(ii) Raf-1 kinase assay. Endogenous Raf-1 was immunoprecipitated from HEK293 cells lysed in Tris-Triton lysis buffer (14) with anti-Raf-1 antibody and protein A-Sepharose. Immunoprecipitates were washed as described above. Truncated activated Raf-1 Δ1-306,Y340/341D (GST–Raf-1 TA) was purchased from Millipore. Kinase assays were performed by using GST-MEK1 (1.0 μg) as a substrate according to the manufacturer's instructions (Millipore).

esiRNA preparation. esiRNA was produced as described previously by Kittler et al. (12). Briefly, using Flag-Nek10 cDNA as a template, 1-kb fragments of Nek10 were PCR amplified with primers containing T7 promoter sequences. The PCR primer sequences for esiNek10#2 were sense primer 5′-CGTAATACGACTCACTATAGGGACTTGAAGCTCCTCTGG-3′ and antisense primer 5′-CGTAATACGACTCACTATAGGGGGATGATAAAGCTGCT-3′, and the PCR primer sequences for esiNek10#3 were sense primer 5′-CGTAATACGACTCACTATAGGGTATGCAATTTTGG-3′ and antisense primer 5′-CGTAATACGACTCACTATAGGGTGTGTGCGTCTTCGTTC-3′. As a control, esiRNA was generated against dsRed.

The PCR product was used as a template for an *in vitro* transcription reaction using a MEGAscript kit (Ambion). The resulting RNA was denatured, annealed, and digested with GST-RNase III (provided by L. Pelletier, Samuel Lunenfeld Research Institute, Toronto, Canada) at 26°C for 5 h, followed by 37°C for 1 h. Digested RNA was purified by using Q-Sepharose.

Semiquantitative PCR. For RNA preparation, cells were harvested, and total RNA was extracted by using an RNeasy minikit (Qiagen). The first-strand cDNA was prepared with 0.5 μg of RNA using qScript cDNA SuperMix (Quanta Biosciences). In preliminary experiments, the relative amounts of cDNA and the range of PCR cycles that permit the linear amplification of Nek10 and β-actin were determined. The PCR primer sequences for Nek10 were sense primer 5′-ATGAGGGATCCATGTTATCAGGAAATAC-3′ and antisense primer 5′-TGGGGCTCTGCACAAAGTA-3′, and those for β-actin were sense primer 5′-GCCAACCGCGAGAAGATGACC-3′ and antisense primer 5′-CTCCTTAATGTCACGCACGATTTC-3′.

The PCR conditions for Nek10 were 94°C for 2 min, followed by 30 cycles of 94°C for 30 s, 55°C for 30 s, and 72°C for 1 min. PCR conditions for β-actin were the same except that the amount of cDNA used as a template was 10 times lower than that for Nek10. Using ImageJ, the relative expression of the Nek10 message was evaluated by calculating the band intensity ratio of Nek10/β-actin.

***In vitro* transcription-translation and *in vitro* binding assays.** Assays were modified from those described previously (29). Briefly, *in vitro* translation was performed by using the Promega TNT T7 Quick Coupled transcription-translation system as described in the kit. Proteins were used immediately and without any purification. For binding reactions, 10 μl Flag-Nek10 transcription-translation reaction mixtures was mixed with 0.5 μg of GST–Raf-1 Δ1-306,Y340/341D (GST–Raf-1 TA) and/or GST-MEK1 (Millipore) in 30 μl of CHAPS lysis buffer and incubated at 30°C for 20 min to allow complex formation. After this incubation, the binding reaction mixtures were diluted with lysis buffer, and immunoprecipitations were carried out with M2 Flag beads at 4°C for 2 h. Immunoprecipitates were washed two times in lysis buffer containing 220 mM NaCl and two times in lysis buffer and were separated by SDS-PAGE.

Flow cytometry. Cell cycle distributions were determined by the flow cytometric analysis of propidium iodide (PI)-labeled cells. Cells were collected, fixed in 70% ethanol, and stored at −20°C overnight. The cells were then washed with phosphate-buffered saline (PBS) and incubated with RNase A and propidium iodide. For quantification of mitotic cells, cells were collected, fixed in 70% ethanol, and stored at −20°C overnight. The cells were washed with PBS and incubated with anti-pS10 H3 antibody (1:1,000; Abcam) for 1 h at room temperature. Cells were washed three times and incubated with anti-mouse antibody–Alexa Fluor 488 (1:250; Molecular Probes) for 30 min at room temperature. Cells were washed one time and incubated with RNase A and propidium iodide. Cell cycle analysis was done by FACScan flow cytometry (BD Biosciences, San Jose, CA).

RESULTS

Cloning and characterization of Nek10, a novel NIMA kinase. A cDNA for Nek10, a previously uncharacterized member of the Nek family, encoding a 1,125-amino-acid (aa) protein, was isolated by PCR from a human skeletal muscle cDNA library. Amino acid sequence alignment within the kinase domain indicates that Nek10 is the most divergent member of the Nek family, sharing 54% homology within this region with its closest mammalian relatives, Nek6 and Nek7. Unlike other Nek kinases that feature N-terminal kinase domains, Nek10 contains a centrally located catalytic domain as well as four N-terminal armadillo repeats (Fig. 1A). In addition, the catalytic domain of Nek10 is flanked by coiled-coiled repeats and a putative PEST sequence near the C terminus. Judged by RT-PCR, Nek10 appears to be ubiquitously expressed at low levels in most mouse tissues, with prominent expression in the mammary gland, lung, spleen, and kidney (Fig. 1B).

Nek10 is a stimulus-specific modulator of ERK1/2. In attempting to define a cellular role for Nek10, we observed that the ectopic expression of Nek10 in HEK293 cells resulted in an increase in the activation-specific phosphorylation of ERK1/2 (data not shown). Curiously, Nek10 expression did not affect

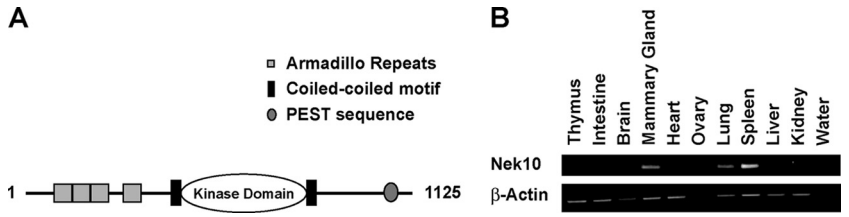

FIG. 1. Cloning and characterization of Nek10, a novel NIMA kinase. (A) Predicted domain structure of full-length Nek10. (B, top) Expression analysis of Nek10 in adult mouse tissues by RT-PCR. (Bottom) Expression analysis of β-actin was used as a control.

ERK1/2 phosphorylation elicited by mitogenic stimuli, such as epidermal growth factor (EGF) (Fig. 2A). Moreover, Nek10 expression did not affect ERK1/2 stimulation by phorbol 12-myristate 13-acetate (PMA) or lysophosphatidic acid (LPA) (data not shown) but did enhance ERK1/2 phosphorylation in response to UV irradiation (Fig. 2A). The effect of Nek10 expression on ERK1/2 activation was dependent on MEK1/2 activity, as it was sensitive to the pretreatment of cells with the

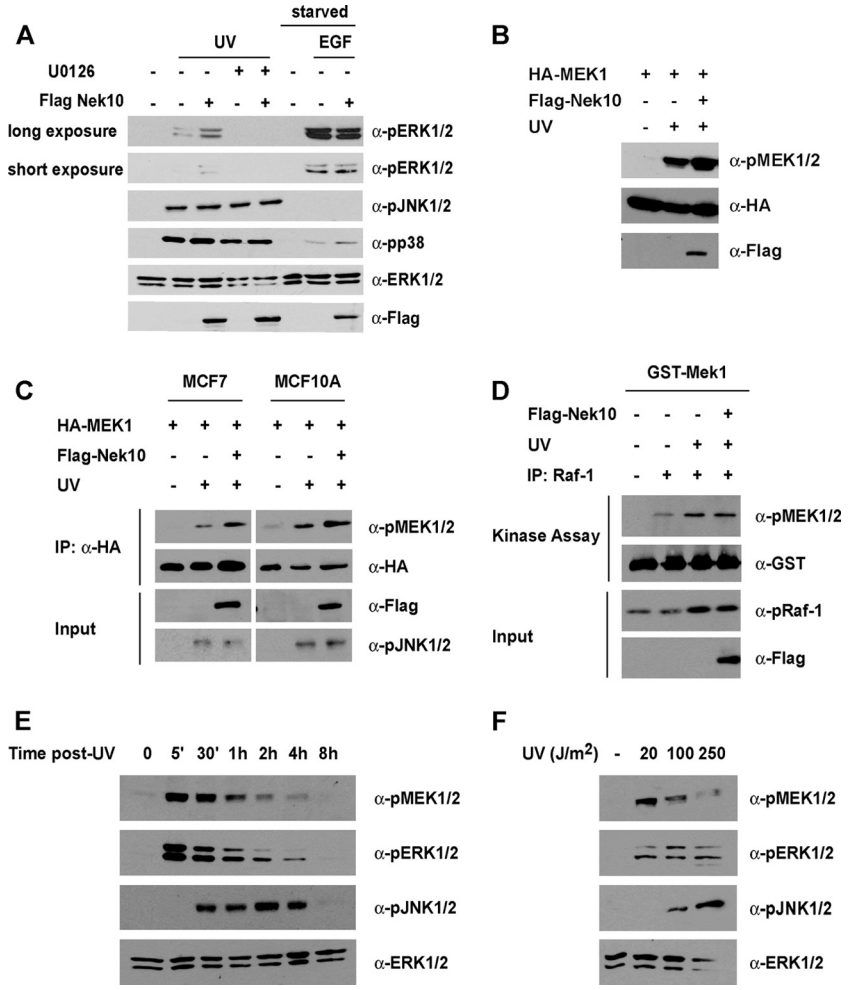

FIG. 2. Nek10 is a stimulus-specific modulator of ERK1/2. (A) Nek10 enhances ERK1/2 activation in response to specific stimuli. HEK293 cells were transfected with Flag-Nek10 and treated with UV (250 J/m^2) or EGF (1 ng/ml) for 30 min before lysis. U0126-treated cells were incubated with U0126 (20 μM) for 1 h prior to UV irradiation. Lysates were immunoblotted as indicated. (B) Nek10 enhances UV-induced MEK1 activation. HEK293 cells were transfected with the indicated constructs and treated with UV (250 J/m^2) for 30 min before lysis. Lysates were immunoblotted as indicated. (C) Nek10 enhances UV-induced MEK1 activation in MCF7 and MCF10A cells. Cells were transfected with the indicated constructs and treated with UV (250 J/m^2) for 30 min before lysis. HA-MEK1 immunoprecipitates (IP) were separated by SDS-PAGE and immunoblotted as indicated. Whole-cell lysates were run as an input control. (D) Nek10 does not affect Raf-1 activity following UV irradiation. HEK293 cells were transfected with the indicated constructs. Cells were treated with UV (250 J/m^2) for 20 min before lysis. Raf-1 immunoprecipitates were used in *in vitro* kinase assays with 1.0 μg GST-MEK1 as a substrate. The phosphorylation of GST-MEK1 was detected by immunoblotting. Whole-cell lysates were run as an input control. (E) Time course of UV-induced MEK1/2 activation. HEK293 cells were lysed at the indicated times after treatment with UV (250 J/m^2). Lysates were immunoblotted as indicated. (F) Dose response of UV-induced MEK1/2 activation. HEK293 cells were treated with the indicated doses of UV for 30 min before lysis. Lysates were immunoblotted as indicated.

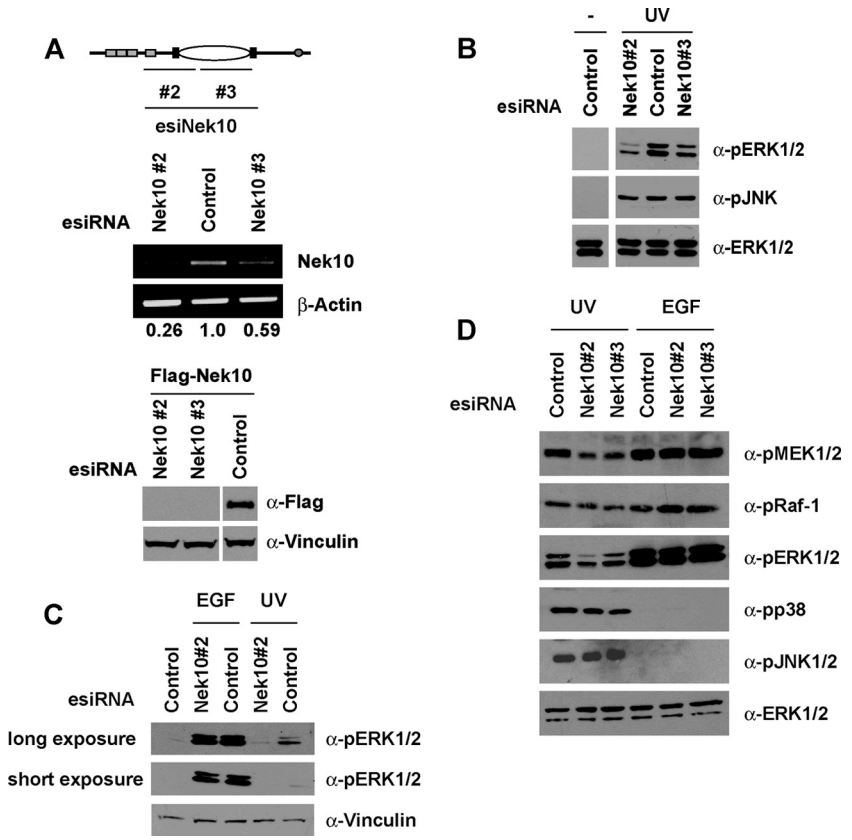

FIG. 3. Nek10 depletion impairs UV-induced MEK1/2 activation. (A) Knockdown of Nek10 in HEK293 cells. HEK293 cells were transfected with pools of esiRNA against Nek10 (top) or dsRed (control), and knockdown was confirmed by semiquantitative RT-PCR (middle). HEK293 cells were cotransfected with pools of esiRNA and Flag-Nek10. Lysates were immunoblotted as indicated (bottom). (B) Knockdown of Nek10 impairs ERK1/2 activation following UV irradiation. HEK293 cells transfected with esiRNA were UV irradiated (250 J/m^2) and harvested 30 min later. Lysates were immunoblotted as indicated. (C) Knockdown of Nek10 does not affect mitogenic ERK1/2 activation. HEK293 cells transfected with esiRNA were UV irradiated (20 J/m^2) or stimulated with EGF (1 ng/ml) and harvested 30 min later. Lysates were immunoblotted as indicated. (D) Knockdown of Nek10 impairs MEK1/2 activation following UV irradiation. HEK293 cells transfected with esiRNA were UV irradiated (250 J/m^2) or stimulated with EGF (0.1 ng/ml) and harvested 30 min later. Lysates were immunoblotted as indicated.

MEK1/2 inhibitor U0126 (Fig. 2A). Two other mitogen-activated protein kinase (MAPK) subfamilies, JNK/SAPK and p38, are known to be robustly activated by stress stimuli, including UV irradiation (reviewed in reference 28). Nevertheless, Nek10 expression did not enhance the activation-specific phosphorylation of JNK or p38 following UV irradiation (Fig. 2A).

Mitogenic stimulation leads to ERK1/2 activation by phosphorylation within its activation loop by the dual-specificity kinases MEK1 and MEK2, which are themselves activated by phosphorylation by the serine/threonine kinase Raf-1 (reviewed in reference 28). We investigated if Nek10 affected the activation of Raf-1 and MEK1/2. Judged by activation-specific MEK1 phosphorylation at S217/S221, cells ectopically expressing Nek10 displayed an enhanced activation of MEK1 following UV irradiation (Fig. 2B). Similarly, the expression of Nek10 in the human breast cancer cell line MCF7 and the untransformed mammary epithelial cell line MCF10A led to activation-specific MEK1 phosphorylation (Fig. 2C). Significantly, although activation-specific Raf-1 S338 phosphorylation was increased following UV irradiation, Nek10 expression did not enhance Raf-1 activity, as measured by an *in vitro* kinase assay (Fig. 2D). Notably, ERK and MEK1/2 activation in response to UV was seen within 5 min of exposure (Fig. 2E) and at all the tested doses (Fig. 2F).

The requirement for Nek10 in ERK1/2 activation was examined with HEK293 cells depleted of Nek10. To do this, esiRNAs against two distinct regions of the human Nek10 cDNA were generated (Fig. 3A, top). HEK293 cells were transfected with Nek10 esiRNA or dsRed esiRNA as a control, and the efficiency of knockdown was determined by RT-PCR. While both of the Nek10 esiRNA pools successfully decreased the level of endogenous Nek10 transcript, esiNek10#2 consistently produced a greater knockdown, resulting in up to a 70% decrease compared to controls (Fig. 3A, middle). Both Nek10 esiRNAs efficiently reduced the expression of the transfected Flag-Nek10 protein, further demonstrating their specificity for the Nek10 mRNA and protein (Fig. 3A, bottom). Our numerous attempts at generating an anti-Nek10 antibody as well as the testing of several commercially available anti-Nek10 antibodies failed to demonstrate a specificity of any of the raised antisera against Nek10 (not shown), precluding the assessment of the efficiency of Nek10 knockdown at the protein level. Nevertheless, the transfection of both Nek10 esiRNAs im-

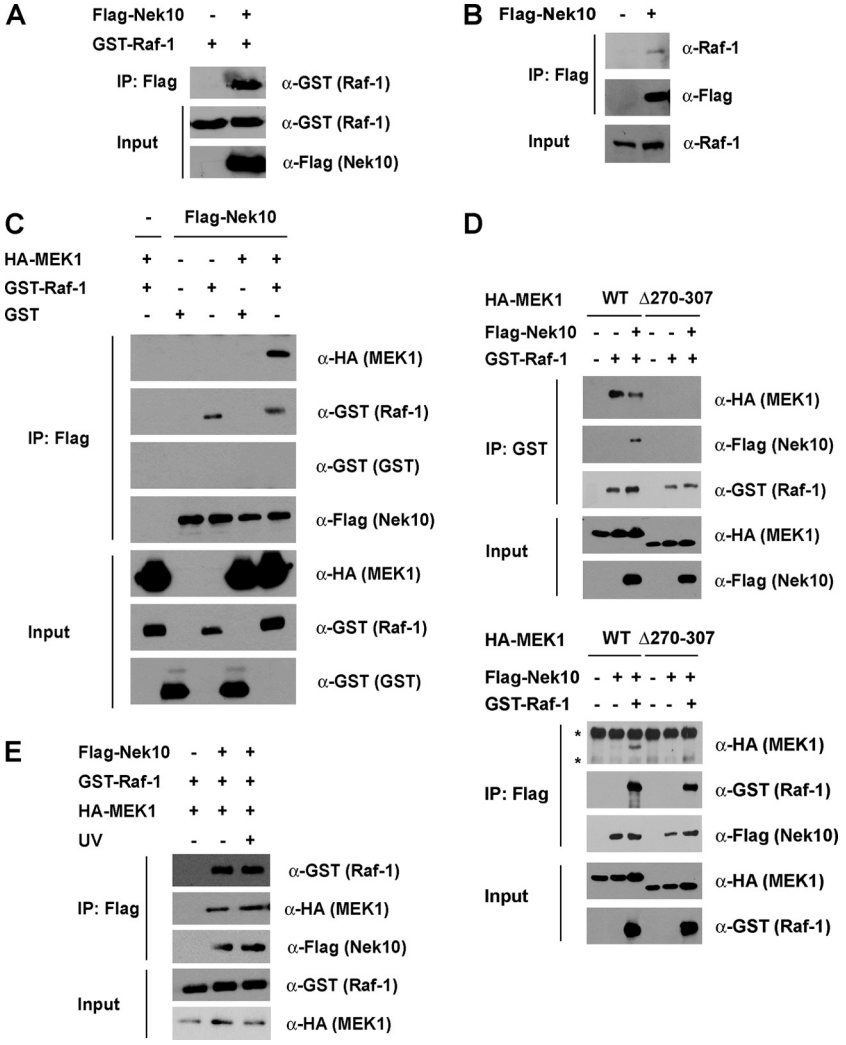

FIG. 4. Nek10 interacts with the Raf-1–MEK1 complex. (A) Nek10 coimmunoprecipitates with Raf-1. HEK293 cells were transfected with the indicated constructs. Nek10 was immunoprecipitated with M2 Flag agarose. Coprecipitated GST–Raf-1 was detected by immunoblotting of the immunoprecipitates. Whole-cell lysates were run as input controls. (B) Nek10 coimmunoprecipitates with endogenous Raf-1. HEK293 cells were transfected with either vector control or Flag-Nek10. Nek10 was immunoprecipitated with M2 Flag agarose. Coprecipitated Raf-1 was detected by immunoblotting of immunoprecipitates with anti-Raf-1 antibody. Whole-cell lysates were run as input controls. (C) Coimmunoprecipitation of Nek10 with Raf-1 and MEK1. HEK293 cells were transfected with the indicated constructs. Protein precipitation and immunodetection were performed as described above for panel A. (D) Raf-1 mediates the assembly of a complex between Nek10, MEK1, and Raf-1. HEK293 cells were transfected with the indicated constructs. Raf-1 was precipitated with glutathione-Sepharose (top), and Nek10 was precipitated with M2 Flag agarose (bottom). Coprecipitating proteins were detected by immunoblotting with the indicated antibodies. Whole-cell lysates were run as input controls. Asterisks indicate nonspecific bands. WT, wild type. (E) The Nek10 interaction with Raf/MEK is not modulated by UV irradiation. HEK293 cells were transfected with the indicated constructs. Cells were UV irradiated (250 J/m^2) 30 min prior to lysis. Protein precipitation and immunodetection were performed as described above for panel A.

paired ERK1/2 activation following both high (250 J/m^2) and low (20 J/m^2) doses of UV irradiation (Fig. 3B and C). Contrary to Nek10 overexpression (Fig. 2B), the depletion of Nek10 resulted in a marked inhibition of UV-stimulated MEK1/2 but not Raf-1, JNK, or p38 phosphorylation (Fig. 3D). Finally, we assessed a role for Nek10 as a stimulus-specific modulator of MEK/ERK. The depletion of Nek10 did not affect ERK1/2 activation following stimulation with EGF (Fig. 3C). Even in response to reduced EGF concentrations, which achieve levels of ERK1/2 activation comparable to that produced by UV irradiation, Nek10 depletion impaired UV- but not EGF-stimulated MEK1/2 and ERK1/2 phosphorylation (Fig. 3D). Thus, Nek10 appears to specifically mediate ERK1/2 activation in response to UV irradiation.

Nek10, Raf-1, and MEK1 form a ternary complex. To probe the mechanism of MEK/ERK activation by Nek10, its ability to directly interact with components of the ERK1/2 signaling cascade was examined. Flag-Nek10 coprecipitated with both GST–Raf-1 from transfected HEK293 cells (Fig. 4A) and endogenous Raf-1 (Fig. 4B). A possible association of Nek10 with MEK1 was also tested. Interestingly, a robust association of Nek10 and MEK1 was observed only upon the coexpression of GST–Raf-1, suggesting that Raf-1 may stabilize an otherwise weak association between Nek10 and MEK1 or may

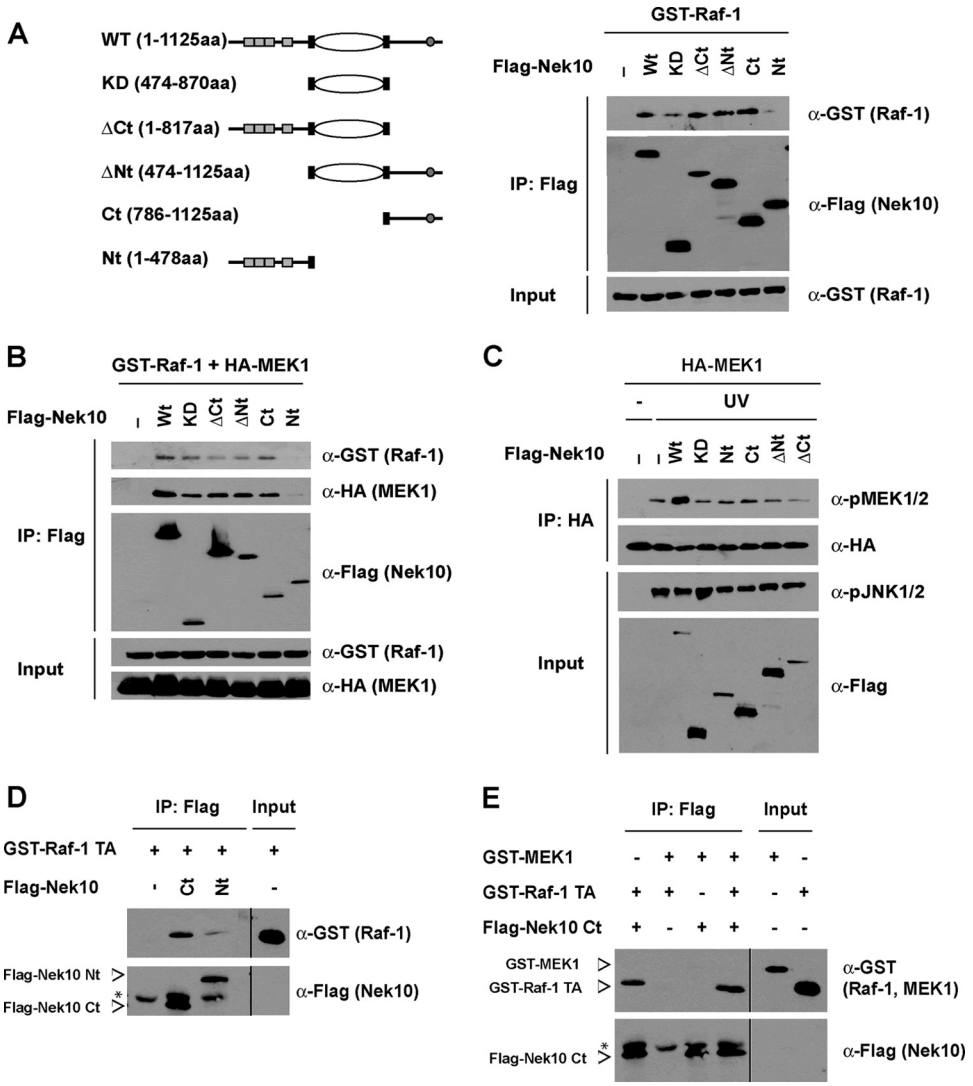

FIG. 5. Nek10 and Raf-1 exhibit a multisite interaction. (A and B) Schematic representation of Nek10 constructs depicting full-length Nek10 and the truncated Nek10 fragments. HEK293 cells were transfected with the indicated constructs. Nek10 was immunoprecipitated with M2 Flag agarose (A, left). Coprecipitated GST–Raf-1 (A, right) or GST–Raf-1/HA-MEK1 (B) was detected by immunoblotting of immunoprecipitates. Whole-cell lysates were run as input controls. (C) Full-length Nek10 promotes UV-induced MEK1 phosphorylation. HEK293 cells transfected with the indicated constructs were treated with UV (250 J/m^2) for 30 min before lysis. HA-MEK1 immunoprecipitates were separated by SDS-PAGE and immunoblotted as indicated. Whole-cell lysates were run as an input control. (D) Nek10 binds Raf-1 *in vitro*. Flag-Nek10 proteins were produced by coupled *in vitro* transcription-translation, incubated with recombinant GST–Raf-1 TA, and immunoprecipitated with M2 Flag agarose. Immunoprecipitates were separated by SDS-PAGE and blotted with the indicated antibodies. A total of 12.5% of the total input of GST–Raf-1 was run as an input control. Asterisks indicate nonspecific bands. (E) Nek10 does not interact with MEK1 *in vitro*. Flag-Nek10 Ct was produced by coupled *in vitro* transcription-translation and incubated with recombinant GST–Raf-1 TA and GST-MEK1. Immunoprecipitation and immunoblotting were performed as described above for panel D. Asterisks indicate nonspecific bands.

bridge the formation of a complex between Nek10 and MEK1 (Fig. 4C). To explore this further, we used a previously characterized MEK1 mutant, MEK1 Δ270-307, which lacks its proline-rich repeat and is unable to interact with Raf-1 (6) (Fig. 4D, top). Upon coexpression, Nek10 associated with the wild type, but not MEK1 Δ270-307, in a Raf-1-dependent manner, further demonstrating that the association between Nek10 and MEK1 requires Raf-1 binding to MEK1 (Fig. 4D, bottom). Of note, the association between Nek10 and Raf-1 was weakened by the expression of MEK1 Δ270-307, suggesting that MEK1 may contribute to the stability of the Nek10/Raf-1 interaction (Fig. 4D). A robust interaction of Nek10 with ectopically expressed ERK2, either alone or in the presence of coexpressed GST–Raf-1, was not detected (data not shown). Interestingly, a ternary complex containing Nek10, Raf-1, and MEK1 formed in the absence of specific cell stimulation and was not modulated upon UV irradiation (Fig. 4E).

To map the interaction between Raf-1 and Nek10, we designed a series of Nek10 deletion mutants and tested their abilities to interact with Raf-1 and MEK1 (Fig. 5A and B). All of the generated mutants retained the ability to interact with Raf-1 and MEK1, except for the Nek10 protein composed of

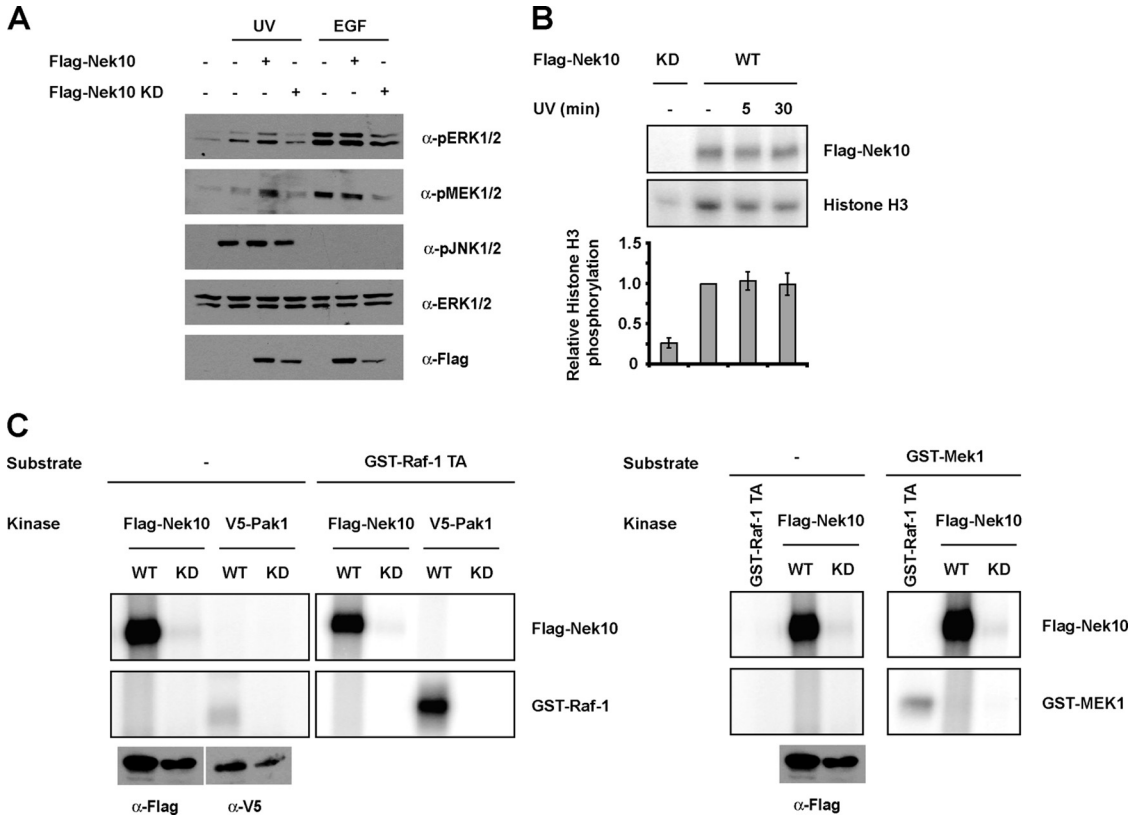

FIG. 6. Nek10 catalytic activity indirectly promotes UV-induced MEK1 activity. (A) Nek10 requires catalytic activity to enhance MEK1 catalytic activity. HEK293 cells were transfected with the indicated constructs. Cells were UV irradiated (250 J/m^2) or stimulated with EGF (0.1 ng/ml) and harvested 30 min later. Lysates were immunoblotted as indicated. (B) Nek10 catalytic activity is not modulated by UV irradiation. HEK293 cells were transfected with the indicated constructs. Cells were lysed at the indicated times after UV irradiation (250 J/m^2), and Nek10 was immunoprecipitated with M2 Flag agarose. Immunoprecipitates were subjected to an *in vitro* kinase assay with histone H3 as a substrate. (Top) Kinase assay mixtures were separated by SDS-PAGE and detected by autoradiography. (Bottom) The results from three independent experiments were quantified. Histone H3 phosphate incorporation was normalized against whole-cell levels of Flag-Nek10. Error bars represent standard errors of the means (SEM). (C) Nek10 does not phosphorylate Raf-1 or MEK1 *in vitro*. HEK293 cells were transfected with wild-type (WT) or kinase-dead (KD) Flag-Nek10 or V5-Pak1. Flag-Nek10 and V5-Pak1 immunoprecipitates or GST–Raf-1 TA (0.1 μg) were used in *in vitro* kinase assays with GST–Raf-1 TA (0.4 μg) (left) or GST-MEK1 (1.0 μg) (right) as a substrate. Kinase assay mixtures were separated by SDS-PAGE, and phosphorylation was detected by autoradiography.

amino acids 1 to 478 encompassing the N-terminal one-third of the protein, which includes the armadillo repeats (Flag-Nek10 Nt) (Fig. 5A and B) indicative of a multisite interaction between Nek10 and Raf-1. Interestingly, although all proteins were able to interact with Raf-1 and MEK1, only full-length Nek10 enhanced MEK1 activation following UV irradiation (Fig. 5C).

To further explore the relationship between Nek10, Raf-1, and MEK1, we examined their interactions *in vitro* using recombinant proteins. The C-terminal portion of Nek10 (Flag-Nek10 Ct), which can interact with Raf-1 and MEK1 (Fig. 5B), and Flag-Nek10 Nt were produced by *in vitro* transcription-translation. Consistent with the above-described results, Flag-Nek10 Ct readily interacted with recombinant GST–Raf-1 Δ1-306,Y340/341D (GST–Raf-1 TA), while Flag-Nek10 Nt did not (Fig. 5D). Interestingly, under these conditions, we were unable to detect an interaction between Flag-Nek10 Ct and recombinant GST-MEK1 either in the presence or in the absence of Raf-1 (Fig. 5E), raising the possibility that additional proteins or posttranslational modifications found in intact cells were required for the Nek10-MEK1 association. Nevertheless, our data strongly indicates that Nek10 interacts directly with Raf-1 to impact ERK signaling.

UV irradiation promotes MEK1 autophosphorylation. The ability of Nek10 to enhance MEK1/2 but not Raf-1 activation following UV irradiation (Fig. 2B and C), combined with the lack of any apparent effect of Nek10 on the Raf-1/MEK1 association (Fig. 4D), prompted us to further explore the mechanism(s) by which Nek10 impacts MEK activity. Considering that Nek10 catalytic activity was required for its effect on MEK phosphorylation upon UV irradiation (Fig. 6A), we examined whether Raf-1 or MEK1/2 was a target of direct phosphorylation by Nek10 (Fig. 6C). While Flag-Nek10 immunoprecipitated from HEK293 cells readily autophosphorylated and phosphorylated the generic serine/threonine kinase substrate histone H3 (Fig. 6B), indicative of its considerable tonic kinase activity, it failed to phosphorylate both Raf-1 and MEK1 *in vitro* (Fig. 6C). Raf-1 and MEK1 were phosphorylated by their well-established upstream kinases Pak1 and Raf-1, respectively, used here as positive controls (Fig. 6C).

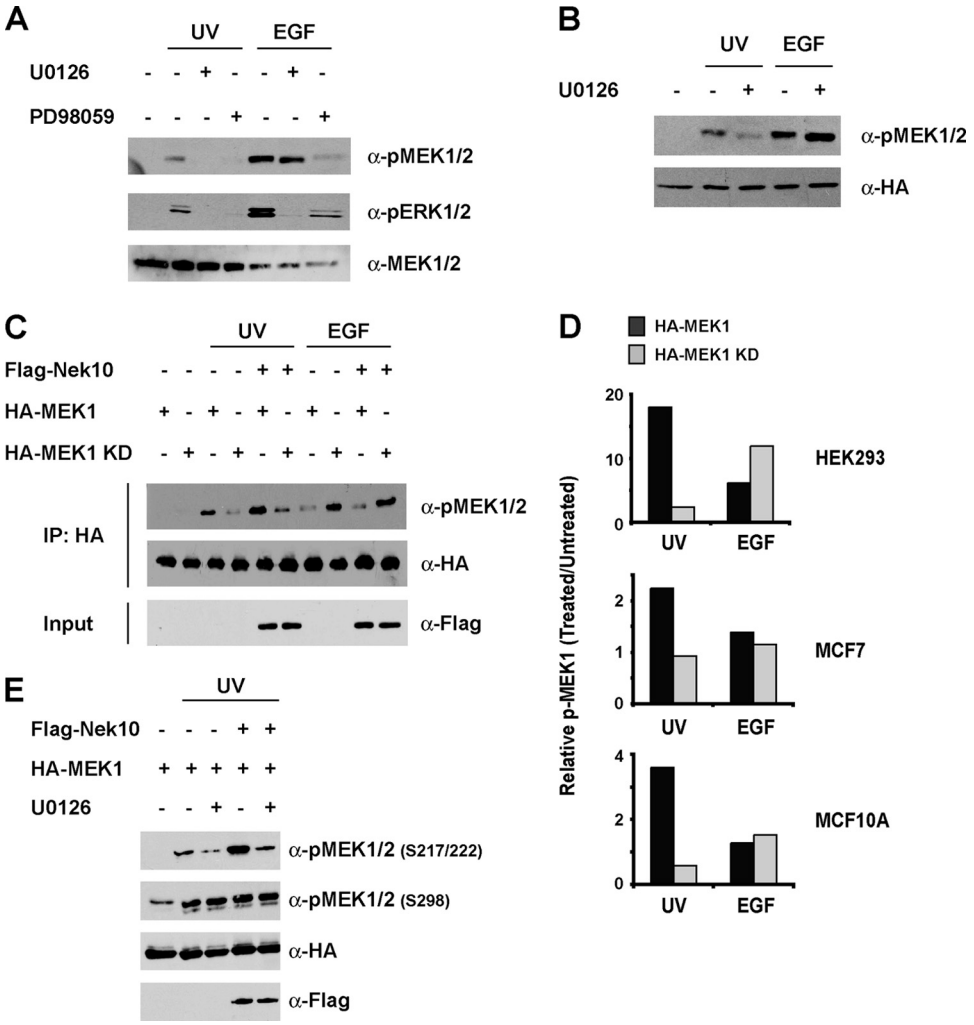

FIG. 7. Nek10 promotes MEK1 autophosphorylation following UV irradiation. (A) UV irradiation stimulates MEK1 autocatalytic activity. HEK293 cells were treated with U0126 (20 μM) or PD98059 (500 μM) for 1 h prior to UV (250 J/m^2) or EGF (1 ng/ml) treatment. Cells were lysed 30 min later. Lysates were immunoblotted as indicated. (B) UV-stimulated MEK1 phosphorylation is sensitive to inhibition of MEK1/2 catalytic activity. HEK293 cells transfected with HA-MEK1 were treated with UV (250 J/m^2) or EGF (0.5 ng/ml) in the presence or absence of U0126 (20 μM). Cells were lysed 30 min later, and lysates were immunoblotted as indicated. (C) MEK1 requires catalytic activity for activation loop phosphorylation following UV irradiation. HEK293 cells were transfected with the indicated constructs and treated with UV (250 J/m^2) or EGF (0.1 ng/ml). Cells were lysed 30 min later. HA-MEK1 was immunoprecipitated, and immunoprecipitates were probed with the indicated antibodies. Whole-cell lysates were run as input controls. (D) MEK1 catalytic activity is required for UV-induced activation loop phosphorylation in MCF7 and MCF10A cells. Cells were transfected with wild-type or kinase-dead (KD) HA-MEK1. HA-MEK1 was immunoprecipitated from cells treated with UV (250 J/m^2) or EGF (0.1 ng/ml). Immunoprecipitates were separated by SDS-PAGE and immunoblotted with the indicated antibodies. Whole-cell lysates were run as input controls. Levels of MEK1 phosphorylation were quantified by ImageJ and normalized against levels of HA-MEK1. Results are expressed relative to levels of pMEK1 in untreated samples. (E) Nek10 promotes U0126-sensitive MEK1 activation following UV irradiation. HEK293 cells were transfected with the indicated constructs and treated with U0126 (20 μM) for 1 h prior to UV irradiation (250 J/m^2). Cells were lysed 30 min following irradiation, and lysates were immunoblotted as indicated.

Significantly, Nek10 kinase activity was not modulated following UV irradiation (Fig. 6B), suggesting that Nek10 catalytic function indirectly contributes to the activation of MEK1/2 by UV, likely via autophosphorylation, contributions to an appropriate protein conformation, and/or interactions with additional proteins.

Using two MEK1/2 inhibitors with different modes of action, we next examined the possible role of autophosphorylation in MEK1/2 activation following UV irradiation. Interestingly, U0126, a direct inhibitor of MEK1/2 catalytic activity, impaired UV- but not EGF-induced MEK1/2 activation loop phosphorylation (Fig. 7A) (2, 9), whereas PD98059, which acts by binding and sequestering inactive forms of MEK (2), affected activation-specific MEK1/2 phosphorylation in response to both stimuli (Fig. 7A). To further investigate whether this was indicative of a stimulus-specific mode of MEK1 activation or was the result of a dose-dependent response to U0126, the effect of U0126 was explored with cells treated with low concentrations of EGF that led to a level of MEK1 phosphorylation comparable to that produced by UV irradiation. Consistent with a role of autophosphorylation in UV-induced MEK activation, even at lower EGF concentrations, UV-induced, but not EGF-

induced, MEK1 phosphorylation was sensitive to U0126 (Fig. 7B). Furthermore, the phosphorylation of catalytically inactive MEK1 (KD) was impaired compared to that of wild-type MEK1 following UV irradiation but not EGF (Fig. 7C and D). Similar results were also seen for MCF7 and MCF10A cells (Fig. 7D). Of note, in HEK293 cells, MEK1 KD phosphorylation increased following EGF administration, likely due to the differential engagement of negative feedback loops downstream of ERK (5) (see Discussion).

We next assessed the effect of Nek10 on MEK1 phosphorylation. While Nek10 expression did not affect EGF-stimulated MEK1 phosphorylation, it enhanced the UV-induced phosphorylation of wild-type but not KD MEK1 (Fig. 7C). Significantly, Nek10-induced MEK1 phosphorylation was also sensitive to U0126 (Fig. 7E). Taken together, these data reveal a distinct mechanism of MEK activation following UV irradiation that requires MEK autocatalytic activity. Nek10 specifically enhances MEK autoactivation in response to UV but does not promote MEK activation in response to mitogens.

MEK1 autoactivation has been implicated as a noncanonical means of stimulating ERK1/2 signaling, specifically in the context of cell attachment (24). In rat embryo fibroblasts, PAK1 phosphorylation of MEK1 at S298 led to MEK1 autophosphorylation at S217/S222 (24). We examined the requirement for S298 phosphorylation in UV-induced MEK autophosphorylation using a catalytically inactive, dominant negative mutant of Pak1 (Pak1 KR). While MEK1 phosphorylation at S298 was abolished by the expression of Pak1 KR, there was no inhibition of S217/S222 phosphorylation by PAK1 KR following UV irradiation, indicating that MEK autoactivation in this context does not require S298 phosphorylation (Fig. 8A).

The autoactivation of MEK upon UV irradiation raised the possibility that Raf-1 may be dispensable for the MEK/ERK response to this stimulus. Nevertheless, MEK1 Δ270-307, which does not bind to Raf-1, was not phosphorylated upon UV irradiation or concomitant Nek10 overexpression (Fig. 8B), indicating that Raf-1 is required for MEK activation following UV irradiation. Interestingly, Raf-1 catalytic activity was not necessary for this effect, as the ectopic expression of catalytically inactive Raf-1 (KD) enhanced UV-induced MEK phosphorylation (Fig. 8C). Significantly, and consistent with a distinct mechanism of MEK activation in response to mitogenic stimuli, the expression of Raf-1 KD inhibited MEK activation in response to EGF (Fig. 8C). Taken together, these data suggest that Raf-1 plays a noncatalytic role in MEK autoactivation following UV irradiation.

Nek10 participates in the maintenance of the G_2/M checkpoint following UV irradiation. In response to genotoxic stress such as ionizing radiation and the intercalating agent etoposide, ERK1/2 activation is required for appropriate G_2/M arrest (30, 32). While ERK1/2 activation by UV irradiation was previously noted (19, 26, 27), a role for ERK1/2 signaling in regulating the G_2/M checkpoint following UV irradiation is unknown. We explored the cell cycle distribution of HEK293 cells following UV irradiation by propidium iodide (PI) staining and flow cytometry. Twenty-four hours after UV irradiation, a 25% increase in the G_2/M population could be detected, indicative of a G_2/M checkpoint arrest (Fig. 9A). The pretreatment of cells with the MEK1/2 inhibitor U0126 markedly attenuated the G_2/M arrest in HEK293 cells, indicating that ERK1/2 plays a role in the response to UV irradiation (Fig. 9A).

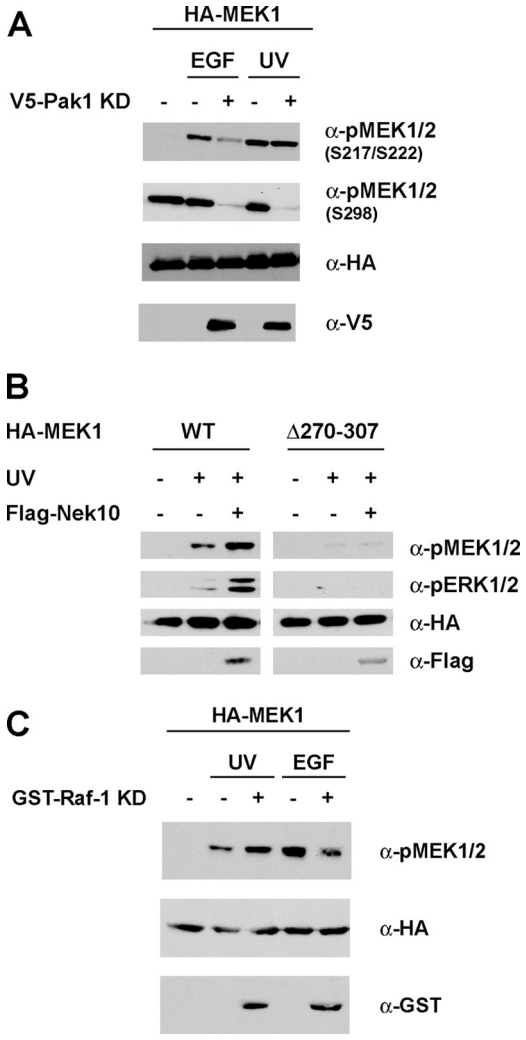

FIG. 8. UV-induced MEK1 autophosphorylation requires Raf-1. (A) S298 phosphorylation is not required for UV-induced MEK1 autoactivation. HEK293 cells were transfected with the indicated constructs and treated with UV (250 J/m^2) or EGF (1 ng/ml). Cells were lysed 30 min later. Lysates were immunoblotted as indicated. (B) Nek10 requires Raf-1 interaction with MEK1 to enhance MEK1 activation. HEK293 cells were transfected with the indicated constructs and treated with UV (250 J/m^2). Cells were lysed 30 min later. Lysates were immunoblotted as indicated. (C) Raf-1 enhances UV-induced MEK1 phosphorylation independent of Raf-1 catalytic activity. HEK293 cells were transfected with the indicated constructs and treated with UV (250 J/m^2) or EGF (0.5 ng/ml). Cells were lysed 30 min later. Lysates were immunoblotted as indicated.

ERK1/2 has a well-established role in promoting G_1 progression (reviewed in reference 18). To ensure that the observed effect of U0126 on the G_2/M checkpoint was not the result of G_1 arrest, we examined the impact of U0126 on synchronized cells that were UV irradiated during the S phase. Briefly, HEK293 cells were synchronized, by mimosine treatment, at the G_1/S phase. Six hours after release from mimosine arrest, cells were UV irradiated and treated with U0126 for 20 h. Importantly, U0126 treatment of nonirradiated cells did

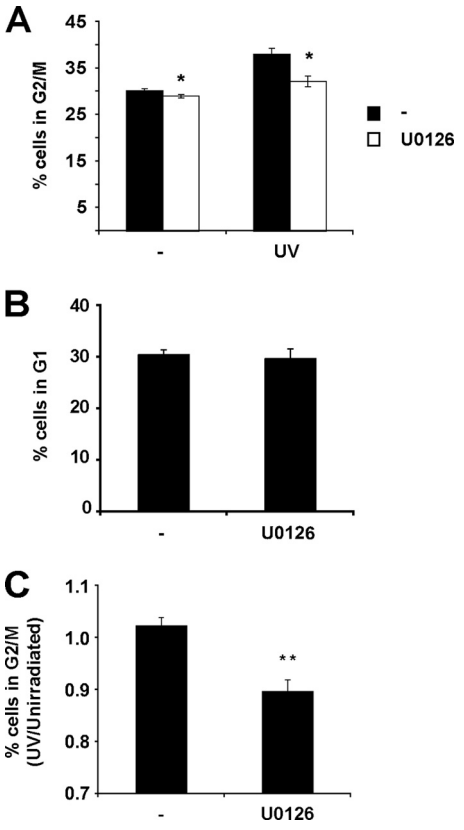

FIG. 9. ERK1/2 activity regulates the UV-induced G_2/M checkpoint. (A) ERK1/2 regulates G_2/M arrest in UV-irradiated cells. HEK293 cells were treated with U0126 (10 μM) starting 1 h prior to UV irradiation (20 J/m^2) and harvested 24 h following irradiation. DNA content was measured by propidium iodide staining. Shown are results from three independent experiments. Error bars represent SEM. *, $P < 0.05$. (B) Effect of U0126 on the G_1 population in synchronized cells. HEK293 cells were synchronized by 24 h of treatment with mimosine (1 mM), washed, and released into fresh medium without mimosine for 6 h. Cells were treated with U0126 (10 μM) and harvested 20 h later. The DNA content was measured by propidium iodide staining. Shown are results from three independent experiments. Error bars represent SEM. (C) ERK1/2 has a role in G_2/M checkpoint control. HEK293 cells were synchronized by 24 h of treatment with mimosine (1 mM), washed, and released into fresh medium without mimosine for 6 h. Cells were UV irradiated (20 J/m^2), treated with U0126 (10 μM), and harvested 20 h later. The DNA content was measured by propidium iodide staining. Shown are results from three independent experiments. The percentage of cells in G_2/M phase is expressed relative to that of nonirradiated samples. Error bars represent SEM. **, $P < 0.005$.

not enrich for G_1-phase cells (Fig. 9B), demonstrating that this method can be used to distinguish between the role of ERK signaling in G_1 cell cycle progression and that at the G_2/M checkpoint. Consistent with our previous observations that ERK signaling also has a role at the G_2/M checkpoint, U0126-treated cells UV irradiated during the S phase displayed a decreased G_2/M population compared to that of control cells (Fig. 9C).

The ability of Nek10 to promote UV-stimulated ERK1/2 activation prompted us to further investigate its function in the UV response. The cell cycle distribution of HEK293 cells depleted of Nek10 by esiRNA was profiled under basal conditions or upon UV irradiation. Following UV irradiation, while the control cells accumulated in G_2/M phase, Nek10-depleted cells were impaired for this response (Fig. 10A and B). Significantly, a similar response was also seen for the nontransformed human mammary epithelial cell line MCF10A (Fig. 10C). Nevertheless, Nek10 depletion did not significantly affect the survival of any of the three tested cell lines (Fig. 10D).

Nek10-depleted cells also displayed an increased proportion of cells in mitosis, as measured by staining for a mitotic marker, the serine 10-phosphorylated histone H3 (pS10 H3). This was most apparent within short time points after UV irradiation (5 h and 10 h) and less prominent at 20 h (Fig. 10F and G). This elevation in numbers of mitotic cells was not due to a defect in normal cell cycle progression, as the depletion of Nek10 led to a small decrease in numbers of mitotic cells under nonirradiated conditions (Fig. 10E). To capture all cells able to escape the G_2/M checkpoint, we treated UV-irradiated cells with nocodazole, a mitotic inhibitor. Interestingly, 20 h after irradiation, there was a significant increase in the proportion of mitotic cells depleted for Nek10, which is further indicative of a continuous defect in the G_2/M arrest upon the loss of Nek10 (Fig. 10E and F). Significantly, esiNek10#2, which displayed greater potency in Nek10 knockdown than esiNek10#3 (Fig. 3A), led to a more severe G_2/M arrest defect (Fig. 10B and 10G), consistent with a dose-dependent effect of the Nek10 knockdown on the UV-induced G_2/M arrest.

DISCUSSION

In this study we demonstrate a role for a novel member of the Nek family, Nek10, in promoting MEK/ERK activation and G_2/M arrest in response to UV irradiation. Our results indicate that Nek10 is a stimulus-specific modulator of ERK1/2 signaling, as its expression enhanced MEK and ERK activation in response to UV irradiation but not to mitogenic stimuli such as EGF (Fig. 2A). Consistent with this, Nek10 depletion led to impaired MEK1/2 and/or ERK1/2 activation in response to UV irradiation but not to EGF stimulation (Fig. 3B and D). Our results indicate that the specificity of the ERK1/2 signaling response to UV can be attributed to the ability of Nek10 to promote a noncanonical mechanism of MEK activation following UV irradiation (Fig. 7E). Interestingly, this mechanism requires MEK catalytic activity (Fig. 7A, B, and C) and Raf-1 binding but not its kinase activity (Fig. 8B and C).

ERK1/2 signaling has traditionally been associated with mitogenic stimulation and the regulation of cell proliferation but is also activated by a diverse range of other stimuli, including cytokines and various stresses, such as UV and ionizing radiation as well as hypoxia (21, 27, 30). One of the means of achieving control in ERK1/2 signaling is the differential interaction of ERK1/2 cascade components with various scaffolding proteins (reviewed in reference 13). These interactions have been found to modulate the stimulus specificity, amplitude, and duration of pathway activation as well as to impact subcellular localization, access to substrates, and cellular outcome (4).

The molecular mechanism by which Nek10 conveys specificity to ERK signaling in the context of UV irradiation remains to be fully elucidated. Nevertheless, Nek10 promotes MEK autoactivation in response to UV but not following EGF stim-

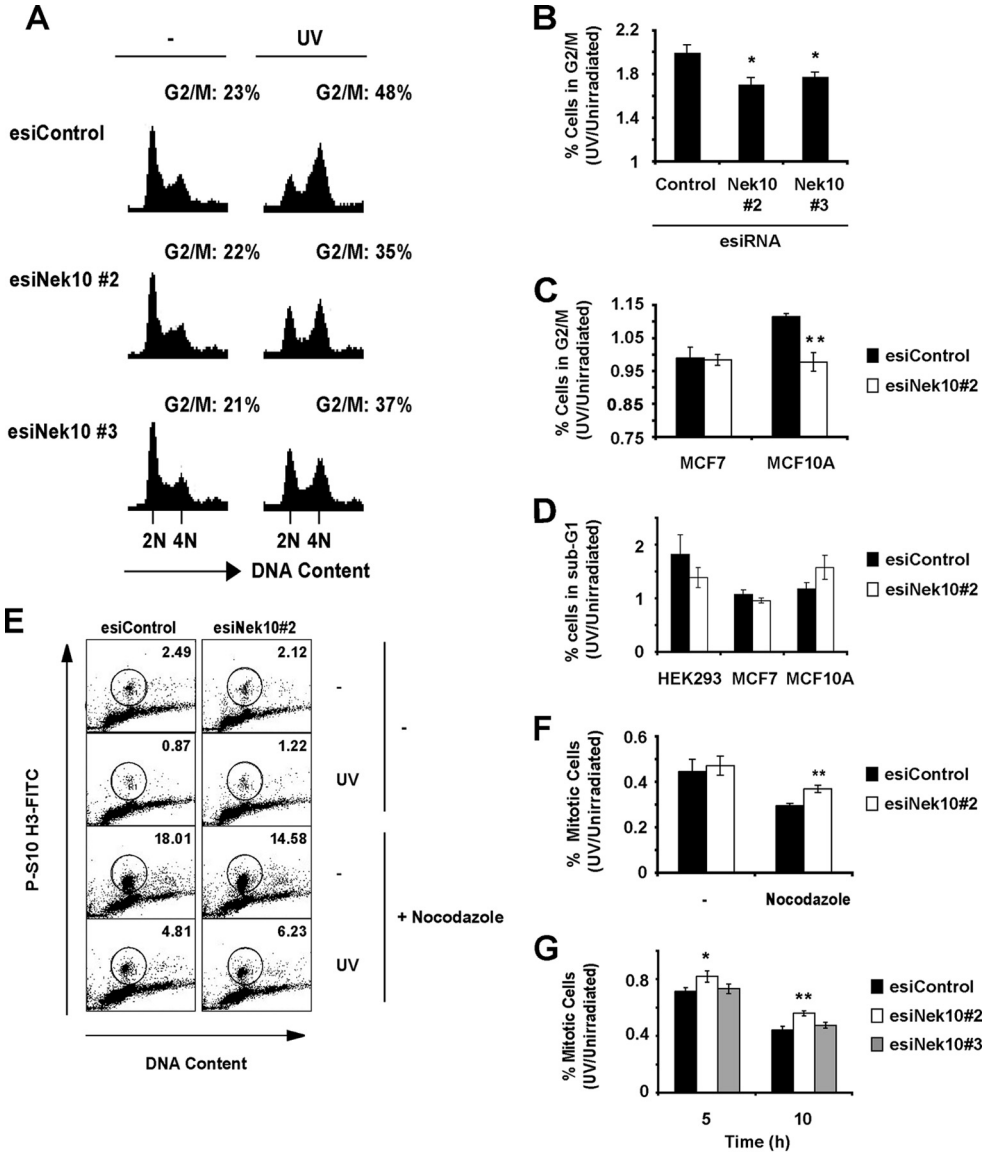

FIG. 10. Nek10 plays a role in maintenance of the G_2/M checkpoint following UV irradiation. (A) Knockdown of Nek10 decreases the G_2/M population in UV-irradiated cells. HEK293 cells were transfected with esiRNA. Cells were treated with UV (20 J/m^2) and harvested 24 h later, and their DNA contents were measured by propidium iodide staining. The proportion of cells in G_2/M phase was quantified. Representative images are shown. (B) Quantitation of G_2/M-phase cells in Nek10 knockdown cells from three independent experiments. The percentage of cells in G_2/M phase is expressed relative to nonirradiated samples. Error bars represent SEM. *, $P < 0.05$. (C) Quantitation of G_2/M-phase cells in Nek10-depleted MCF7 and MCF10A cells. The experiment was performed as described above for A. Shown are the results from three independent experiments. Error bars represent SEM. **, $P < 0.005$. (D) Cell survival of Nek10-depleted cells. Cells transfected with esiRNA were gathered 20 h after UV irradiation (20 J/m^2), and cell cycle profiles were analyzed by PI staining. Cells appearing as sub-G_1-phase cells were scored as apoptotic. Results shown are from three independent experiments. The percentage of sub-G_1 cells is expressed relative to nonirradiated samples. Error bars represent SEM. (E) Nek10-depleted cells progress through mitosis after DNA damage. HEK293 cells were transfected with esiRNA. Cells were UV irradiated (20 J/m^2) and treated with nocodazole (50 ng/ml) 1 h after UV irradiation. Cells were gathered 20 h after UV irradiation, and the percentage of mitotic cells was determined by dual staining with propidium iodide (DNA) and anti-pSer10-H3 (mitotic cells). Representative images are shown. (F) Quantitation of mitotic cells in UV-irradiated esiRNA-transfected cells from three independent experiments. The percentage of mitotic cells is expressed relative to nonirradiated samples. Error bars represent SEM. **, $P < 0.005$. (G) Depletion of Nek10 impairs activation of the G_2/M checkpoint. HEK293 cells were transfected with esiRNA. Cells were gathered at the indicated time points after UV irradiation (20 J/m^2) and processed as described above for panel E. Shown are the results from three independent experiments. The percentage of mitotic cells is expressed relative to nonirradiated samples. Error bars represent SEM. *, $P < 0.05$; **, $P < 0.005$.

ulation (Fig. 7C and E), suggesting a mechanism of MEK regulation distinct from the canonical Ras/Raf/MEK cascade. We demonstrated a role for MEK autoactivation in response to UV irradiation by uncovering a sensitivity of MEK phosphorylation upon this insult to the inhibition of MEK catalytic activity, either by U0126 treatment or by the expression of MEK KD (Fig. 7B and C). Conversely, MEK catalytic activity was not a requisite for MEK phosphorylation following EGF

treatment (Fig. 7B and C). Interestingly, while MEK KD phosphorylation was impaired following UV irradiation, it was enhanced in response to EGF stimulation (Fig. 7C). Considering that MEK1 and MEK2 are subject to ERK-dependent negative feedback regulation, it is likely that the ectopic expression of MEK1 KD prevented the activation of ERK and the engagement of the feedback loop, thus leading to an enhanced/prolonged phosphorylation of MEK1 KD (5). Taken together, these observations highlight the fact that the molecular mechanisms of MEK activation following UV irradiation and EGF stimulation differ. While MEK autoactivation appears to play a dominant role in UV-induced MEK/ERK activation, our data do not exclude the possibility that additional UV-induced regulatory inputs into MEK exist, including phosphatases and yet-to-be-discovered MEK protein-protein interactions.

Significantly, the MEK response to UV irradiation was independent of MEK S298 phosphorylation (Fig. 8A), which was previously implicated in MEK autoactivation in the context of cell adhesion (24). Our data are consistent with the formation of a MEK autoactivation-competent complex consisting of Nek10, Raf-1, and MEK. Interestingly, while the association of Nek10 with Raf-1 and MEK was needed for enhanced MEK1 activation in response to UV irradiation (Fig. 8B), the formation of the ternary complex was not sensitive to UV irradiation (Fig. 4E). Furthermore, the Raf-1 protein, but not its catalytic activity, was required for MEK1 activation following UV irradiation (Fig. 8C). The ability of Raf-1 to bridge the association between Nek10 and MEK (Fig. 4C) points toward a scaffolding, noncatalytic role for Raf-1 in the formation of the MEK autoactivation complex.

The fact that signaling by the Nek10/Raf/MEK module depends on MEK autocatalysis points toward the existence of distinct spatial and temporal controls for MEK activation in response to specific stimuli. In the case of UV irradiation, Nek10 participation in this complex may promote associations with additional regulators and facilitate a permissive change in the MEK conformation leading to its autoactivation and/or govern access to specific substrates. The uncoupling of MEK activation from receptor tyrosine kinases, Ras, and their other effectors allows for the discrete control of MEK/ERK signaling targets, leading to specific outcomes, such as the engagement of the G_2/M checkpoint in response to UV irradiation (Fig. 9A and 10B).

ERK signaling was previously implicated in the regulation of cell cycle checkpoints in response to ionizing radiation and etoposide in MCF-7 and NIH 3T3 cells, respectively (30, 32, 33). Our results revealed a role for ERK1/2 activation in the engagement of the G_2/M checkpoint following UV irradiation of HEK293 cells (Fig. 9A). A similar phenotype was also observed for UV-irradiated cells depleted of Nek10 by esiRNA (Fig. 10B, F, and G). Moreover, similar to what was previously reported for Nek11, the depletion of Nek10 led to a small decrease in numbers of mitotic cells under nonirradiated conditions (Fig. 10E), indicating that Nek10 may have additional roles in the control of normal cell cycle progression (17). Taken together, our results suggest that Nek10-mediated ERK1/2 activation participates in UV-induced G_2/M arrest. Nevertheless, this does not exclude the possibility that there is an additional defect in DNA repair that may contribute to our observations and may be the subject of future studies.

A possible association of Nek10 function and cancer was recently uncovered by a comprehensive genome-wide association study (GWAS) involving over 37,000 breast cancer samples and over 40,000 controls, which identified a strong breast cancer susceptibility locus within chromosome 3p24 containing only two genes, Nek10 and SLC4A7 (solute carrier family 4, sodium bicarbonate transporter, member 7) (1). Moreover, cancer genome sequencing projects have also reported Nek10 mutations in several human cancers (8, 11). Nek10 was one of only 21 protein kinases in the whole kinome (518 genes) that displayed multiple nonsynonymous somatic mutations within a group of 26 primary lung neoplasms and seven lung cancer cell lines. Remarkably, Nek10 mutations were found with the same frequency (4/33) as the mutations for BRAF and STK11/LKB1, kinases previously implicated in the etiology of lung cancer (8). While Nek10 somatic mutations map to various regions of the protein (R878M in large-cell lung carcinoma, P1115L in lung neuroendocrine carcinoma, A66K in ovarian mucinous carcinoma, and E379K in a metastatic melanoma cell line, etc.), their impact on the integrity of Nek10 proteins is unknown. It would be interesting to determine how these mutations affect the function of Nek10 in the engagement of the G_2/M checkpoint in response to genotoxic stress and provide further insight into the role of Nek10 in tumorigenesis.

ACKNOWLEDGMENTS

We thank Melanie Cobb, Andrew Catling, Jim Woodgett, Peter Cheung, Laurence Pelletier, and David W Hedley for gifts of reagents; W. Brent Derry for the gift of reagents and technical advice; Michelle Li and Jason Ho for technical help; and Peter Cheung, Nadeem Moghal, and Previn Dutt for critical reading of the manuscript.

This work was supported by the Canadian Institute of Health Research (grant COP 107970 to V.S.). L.S.M. is a recipient of the CIHR strategic training fellowship of the EIRR 21st Program.

We declare that we have no conflict of interest.

L.S.M. conducted research, and L.S.M. and V.S. designed research and wrote the paper.

REFERENCES

1. **Ahmed, S., G. Thomas, M. Ghoussaini, C. S. Healey, M. K. Humphreys, R. Platte, J. Morrison, M. Maranian, K. A. Pooley, R. Luben, D. Eccles, D. G. Evans, O. Fletcher, N. Johnson, I. Dos Santos Silva, J. Peto, M. R. Stratton, N. Rahman, K. Jacobs, R. Prentice, G. L. Anderson, A. Rajkovic, J. D. Curb, R. G. Ziegler, C. D. Berg, S. S. Buys, C. A. McCarty, H. S. Feigelson, E. E. Calle, M. J. Thun, W. R. Diver, S. Bojesen, B. G. Nordestgaard, H. Flyger, T. Dork, P. Schurmann, P. Hillemanns, J. H. Karstens, N. V. Bogdanova, N. N. Antonenkova, I. V. Zalutsky, M. Bermisheva, S. Fedorova, E. Khusnutdinova, D. Kang, K. Y. Yoo, D. Y. Noh, S. H. Ahn, P. Devilee, C. J. van Asperen, R. A. Tollenaar, C. Seynaeve, M. Garcia-Closas, J. Lissowska, L. Brinton, B. Peplonska, H. Nevanlinna, T. Heikkinen, K. Aittomaki, C. Blomqvist, J. L. Hopper, M. C. Southey, L. Smith, A. B. Spurdle, M. K. Schmidt, A. Broeks, R. R. van Hien, S. Cornelissen, R. L. Milne, G. Ribas, A. Gonzalez-Neira, J. Benitez, R. K. Schmutzler, B. Burwinkel, C. R. Bartram, A. Meindl, H. Brauch, C. Justenhoven, U. Hamann, J. Chang-Claude, R. Hein, S. Wang-Gohrke, A. Lindblom, S. Margolin, A. Mannermaa, V. M. Kosma, V. Kataja, J. E. Olson, X. Wang, Z. Fredericksen, G. G. Giles, G. Severi, L. Baglietto, D. R. English, S. E. Hankinson, D. G. Cox, P. Kraft, L. J. Vatten, K. Hveem, M. Kumle, et al.** 2009. Newly discovered breast cancer susceptibility loci on 3p24 and 17q23.2. Nat. Genet. **41:**585–590.
2. **Alessi, D. R., A. Cuenda, P. Cohen, D. T. Dudley, and A. R. Saltiel.** 1995. PD 098059 is a specific inhibitor of the activation of mitogen-activated protein kinase kinase in vitro and in vivo. J. Biol. Chem. **270:**27489–27494.
3. **Bulavin, D. V., Y. Higashimoto, I. J. Popoff, W. A. Gaarde, V. Basrur, O. Potapova, E. Appella, and A. J. Fornace, Jr.** 2001. Initiation of a G2/M checkpoint after ultraviolet radiation requires p38 kinase. Nature **411:**102–107.
4. **Casar, B., I. Arozarena, V. Sanz-Moreno, A. Pinto, L. Agudo-Ibanez, R. Marais, R. E. Lewis, M. T. Berciano, and P. Crespo.** 2009. Ras subcellular localization defines extracellular signal-regulated kinase 1 and 2 substrate specificity through distinct utilization of scaffold proteins. Mol. Cell. Biol. **29:**1338–1353.

5. **Catalanotti, F., G. Reyes, V. Jesenberger, G. Galabova-Kovacs, R. de Matos Simoes, O. Carugo, and M. Baccarini.** 2009. A Mek1-Mek2 heterodimer determines the strength and duration of the Erk signal. Nat. Struct. Mol. Biol. **16:**294–303.
6. **Catling, A. D., H. J. Schaeffer, C. W. Reuter, G. R. Reddy, and M. J. Weber.** 1995. A proline-rich sequence unique to MEK1 and MEK2 is required for raf binding and regulates MEK function. Mol. Cell. Biol. **15:**5214–5225.
7. **Chen, Y., P. L. Chen, C. F. Chen, X. Jiang, and D. J. Riley.** 2008. Never-in-mitosis related kinase 1 functions in DNA damage response and checkpoint control. Cell Cycle **7:**3194–3201.
8. **Davies, H., C. Hunter, R. Smith, P. Stephens, C. Greenman, G. Bignell, J. Teague, A. Butler, S. Edkins, C. Stevens, A. Parker, S. O'Meara, T. Avis, S. Barthorpe, L. Brackenbury, G. Buck, J. Clements, J. Cole, E. Dicks, K. Edwards, S. Forbes, M. Gorton, K. Gray, K. Halliday, R. Harrison, K. Hills, J. Hinton, D. Jones, V. Kosmidou, R. Laman, R. Lugg, A. Menzies, J. Perry, R. Petty, K. Raine, R. Shepherd, A. Small, H. Solomon, Y. Stephens, C. Tofts, J. Varian, A. Webb, S. West, S. Widaa, A. Yates, F. Brasseur, C. S. Cooper, A. M. Flanagan, A. Green, M. Knowles, S. Y. Leung, L. H. Looijenga, B. Malkowicz, M. A. Pierotti, B. T. Teh, S. T. Yuen, S. R. Lakhani, D. F. Easton, B. L. Weber, P. Goldstraw, A. G. Nicholson, R. Wooster, M. R. Stratton, and P. A. Futreal.** 2005. Somatic mutations of the protein kinase gene family in human lung cancer. Cancer Res. **65:**7591–7595.
9. **Favata, M. F., K. Y. Horiuchi, E. J. Manos, A. J. Daulerio, D. A. Stradley, W. S. Feeser, D. E. Van Dyk, W. J. Pitts, R. A. Earl, F. Hobbs, R. A. Copeland, R. L. Magolda, P. A. Scherle, and J. M. Trzaskos.** 1998. Identification of a novel inhibitor of mitogen-activated protein kinase kinase. J. Biol. Chem. **273:**18623–18632.
10. **Fletcher, L., G. J. Cerniglia, E. A. Nigg, T. J. Yend, and R. J. Muschel.** 2004. Inhibition of centrosome separation after DNA damage: a role for Nek2. Radiat. Res. **162:**128–135.
11. **Greenman, C., P. Stephens, R. Smith, G. L. Dalgliesh, C. Hunter, G. Bignell, H. Davies, J. Teague, A. Butler, C. Stevens, S. Edkins, S. O'Meara, I. Vastrik, E. E. Schmidt, T. Avis, S. Barthorpe, G. Bhamra, G. Buck, B. Choudhury, J. Clements, J. Cole, E. Dicks, S. Forbes, K. Gray, K. Halliday, R. Harrison, K. Hills, J. Hinton, A. Jenkinson, D. Jones, A. Menzies, T. Mironenko, J. Perry, K. Raine, D. Richardson, R. Shepherd, A. Small, C. Tofts, J. Varian, T. Webb, S. West, S. Widaa, A. Yates, D. P. Cahill, D. N. Louis, P. Goldstraw, A. G. Nicholson, F. Brasseur, L. Looijenga, B. L. Weber, Y. E. Chiew, A. DeFazio, M. F. Greaves, A. R. Green, P. Campbell, E. Birney, D. F. Easton, G. Chenevix-Trench, M. H. Tan, S. K. Khoo, B. T. Teh, S. T. Yuen, S. Y. Leung, R. Wooster, P. A. Futreal, and M. R. Stratton.** 2007. Patterns of somatic mutation in human cancer genomes. Nature **446:**153–158.
12. **Kittler, R., A. K. Heninger, K. Franke, B. Habermann, and F. Buchholz.** 2005. Production of endoribonuclease-prepared short interfering RNAs for gene silencing in mammalian cells. Nat. Methods **2:**779–784.
13. **Kolch, W.** 2005. Coordinating ERK/MAPK signalling through scaffolds and inhibitors. Nat. Rev. Mol. Cell Biol. **6:**827–837.
14. **Lambert, J. M., Q. T. Lambert, G. W. Reuther, A. Malliri, D. P. Siderovski, J. Sondek, J. G. Collard, and C. J. Der.** 2002. Tiam1 mediates Ras activation of Rac by a PI(3)K-independent mechanism. Nat. Cell Biol. **4:**621–625.
15. **Lee, M. Y., H. J. Kim, M. A. Kim, H. J. Jee, A. J. Kim, Y. S. Bae, J. I. Park, J. H. Chung, and J. Yun.** 2008. Nek6 is involved in G2/M phase cell cycle arrest through DNA damage-induced phosphorylation. Cell Cycle **7:**2705–2709.
16. **Manning, G., D. B. Whyte, R. Martinez, T. Hunter, and S. Sudarsanam.** 2002. The protein kinase complement of the human genome. Science **298:**1912–1934.
17. **Melixetian, M., D. K. Klein, C. S. Sorensen, and K. Helin.** 2009. NEK11 regulates CDC25A degradation and the IR-induced G2/M checkpoint. Nat. Cell Biol. **11:**1247–1253.
18. **Meloche, S., and J. Pouyssegur.** 2007. The ERK1/2 mitogen-activated protein kinase pathway as a master regulator of the G1- to S-phase transition. Oncogene **26:**3227–3239.
19. **Merienne, K., S. Jacquot, M. Zeniou, S. Pannetier, P. Sassone-Corsi, and A. Hanauer.** 2000. Activation of RSK by UV-light: phosphorylation dynamics and involvement of the MAPK pathway. Oncogene **19:**4221–4229.
20. **Mi, J., C. Guo, D. L. Brautigan, and J. M. Larner.** 2007. Protein phosphatase-1alpha regulates centrosome splitting through Nek2. Cancer Res. **67:**1082–1089.
21. **Minet, E., T. Arnould, G. Michel, I. Roland, D. Mottet, M. Raes, J. Remacle, and C. Michiels.** 2000. ERK activation upon hypoxia: involvement in HIF-1 activation. FEBS Lett. **468:**53–58.
22. **Noguchi, K., H. Fukazawa, Y. Murakami, and Y. Uehara.** 2002. Nek11, a new member of the NIMA family of kinases, involved in DNA replication and genotoxic stress responses. J. Biol. Chem. **277:**39655–39665.
23. **Oakley, B. R., and N. R. Morris.** 1983. A mutation in Aspergillus nidulans that blocks the transition from interphase to prophase. J. Cell Biol. **96:**1155–1158.
24. **Park, E. R., S. T. Eblen, and A. D. Catling.** 2007. MEK1 activation by PAK: a novel mechanism. Cell. Signal. **19:**1488–1496.
25. **Polci, R., A. Peng, P. L. Chen, D. J. Riley, and Y. Chen.** 2004. NIMA-related protein kinase 1 is involved early in the ionizing radiation-induced DNA damage response. Cancer Res. **64:**8800–8803.
26. **Price, M. A., F. H. Cruzalegui, and R. Treisman.** 1996. The p38 and ERK MAP kinase pathways cooperate to activate ternary complex factors and c-fos transcription in response to UV light. EMBO J. **15:**6552–6563.
27. **Radler-Pohl, A., C. Sachsenmaier, S. Gebel, H. P. Auer, J. T. Bruder, U. Rapp, P. Angel, H. J. Rahmsdorf, and P. Herrlich.** 1993. UV-induced activation of AP-1 involves obligatory extranuclear steps including Raf-1 kinase. EMBO J. **12:**1005–1012.
28. **Roux, P. P., and J. Blenis.** 2004. ERK and p38 MAPK-activated protein kinases: a family of protein kinases with diverse biological functions. Microbiol. Mol. Biol. Rev. **68:**320–344.
29. **Rushworth, L. K., A. D. Hindley, E. O'Neill, and W. Kolch.** 2006. Regulation and role of Raf-1/B-Raf heterodimerization. Mol. Cell. Biol. **26:**2262–2272.
30. **Tang, D., D. Wu, A. Hirao, J. M. Lahti, L. Liu, B. Mazza, V. J. Kidd, T. W. Mak, and A. J. Ingram.** 2002. ERK activation mediates cell cycle arrest and apoptosis after DNA damage independently of p53. J. Biol. Chem. **277:**12710–12717.
31. **Wang, X., C. H. McGowan, M. Zhao, L. He, J. S. Downey, C. Fearns, Y. Wang, S. Huang, and J. Han.** 2000. Involvement of the MKK6-p38gamma cascade in gamma-radiation-induced cell cycle arrest. Mol. Cell. Biol. **20:**4543–4552.
32. **Yan, Y., C. P. Black, and K. H. Cowan.** 2007. Irradiation-induced G2/M checkpoint response requires ERK1/2 activation. Oncogene **26:**4689–4698.
33. **Yan, Y., R. S. Spieker, M. Kim, S. M. Stoeger, and K. H. Cowan.** 2005. BRCA1-mediated G2/M cell cycle arrest requires ERK1/2 kinase activation. Oncogene **24:**3285–3296.
34. **Zanke, B. W., K. Boudreau, E. Rubie, E. Winnett, L. A. Tibbles, L. Zon, J. Kyriakis, F. F. Liu, and J. R. Woodgett.** 1996. The stress-activated protein kinase pathway mediates cell death following injury induced by cis-platinum, UV irradiation or heat. Curr. Biol. **6:**606–613.